

# DESIGN OF A SUPERCONDUCTING GANTRY FOR PROTONS

Cristian Bontoiu\*, Jose Sanchez-Segovia, FABIS, Spain  
 Rafael Berjillos, Javier Perez Bermejo, TTI, Spain  
 Ismael Martel, Univ. of Huelva, Spain

## Abstract

The last decade brought much interest in proton therapy within the medical and accelerator communities. Using normal conducting technology, the high-energy beams required can be handled only with large and heavy magnets which causes prohibitive costs. While lattice design work on a superconducting gantry has been carried out for a decade [1] there is yet no practical implementation. The University of Huelva in collaboration with the Andalusian Foundation for Health Research (FABIS) is currently involved in developing and assembling a prototype for a compact superconducting proton gantry [2]. Magnet design and performance is described along with beam dynamics results for the main gantry arcs and for the final spot scanning system using realistic magnetic field maps thoroughly.

## INTRODUCTION

The gantry should operate within as much as possible of the medically relevant energy range 100 MeV to 250 MeV delivering proton bunches of about 1 mm rms transverse size with a beam divergence within 2 mrad. Due to space limitations its optical lattice can be made of combined-function magnets which both bend and focus the beam. Tumour scanning in depth involves change of the beam energy which is quicker than the jumps of current intensity allowed by the superconducting magnets and therefore the lattice must hold beams of variable energies at fixed field. The current lattice is composed of 36 magnets installed on two arcs of 2.5 m radius as shown in Fig. 1.

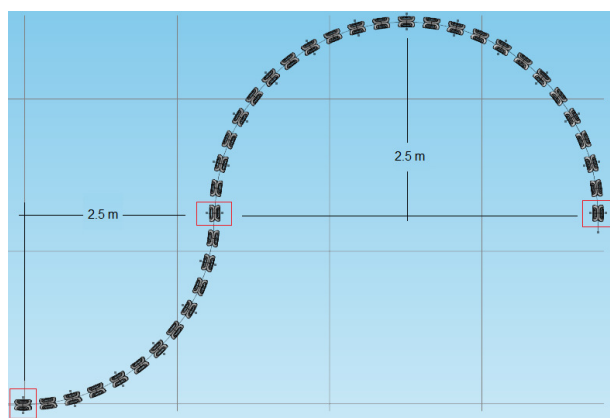


Figure 1: A lattice made of 36 combined-function magnets with the bending radius of 2.5 m.

## MAGNET DESIGN

Successful operation of SC magnets in large scale projects like the LHC, has motivated and inspired the development of a simplified version of combined-function magnets using bent  $\cos-\theta$  dipole and quadrupole coils. They consists of one layer of quadrupole coils installed on the top of one layer of dipole coils, both layers spanning about  $3.5^\circ$  axially. Numerical modelling has been achieved in Comsol [3] resulting in three-dimensional magnetic field maps overlapped, scaled and used for particle tracking studies.

### Dipole Coils

The dipole coils have been designed using three 1 cm thick coil blocks whose azimuthal distribution minimizes the  $b_3, b_5, b_7, b_9, b_{11}$  multipoles as described in [4]. A view is shown in Fig. 2 with the inner radius set at 5 cm.

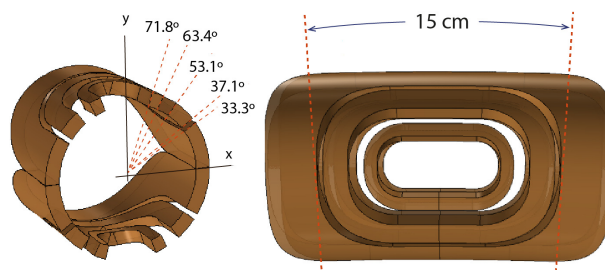


Figure 2: Three-dimensional layout of the SC dipole coils.

The dipole magnetic field is highly homogeneous, as it can be seen across the transverse cross-section in Fig. 3. A current density of about  $350 \text{ A/mm}^2$  is required to handle proton beams of 250 MeV.

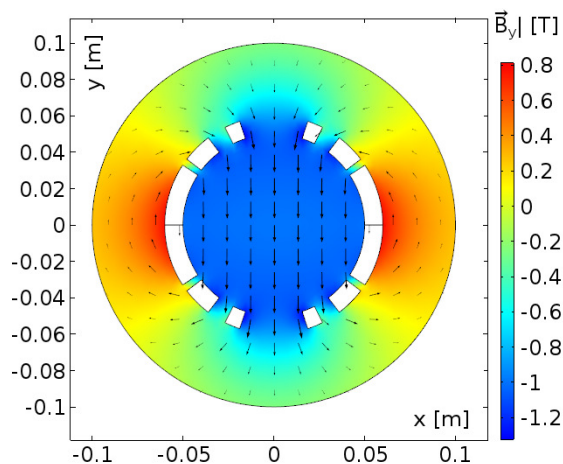


Figure 3: Dipole magnetic field distribution within the transverse cross-section plane.

\* cbontoiu@gmail.com

Content from this work may be used under the terms of the CC BY 3.0 licence (© 2015). Any distribution of this work must maintain attribution to the author(s), title of the work, publisher, and DOI.

## Quadrupole Coils

The quadrupole coils consist of the two blocks shown in Fig. 4. Their particular azimuthal span was chosen in order to minimize the  $b_6$  and  $b_{10}$  multipoles [5].

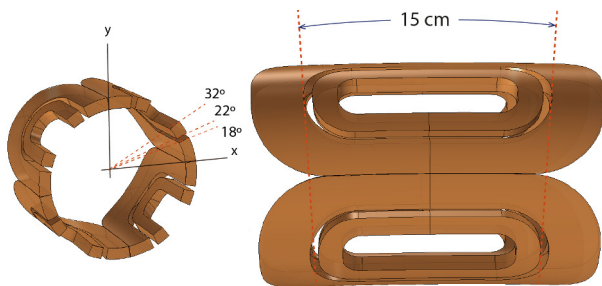


Figure 4: Three-dimensional layout of the SC quadrupole coils.

The field pattern is shown in Fig. 5 for a gradient of 25 T/m. At the highest proton energy of 250 MeV the required gradient is  $\sim 90$  T/m which needs 975 A/mm<sup>2</sup>.

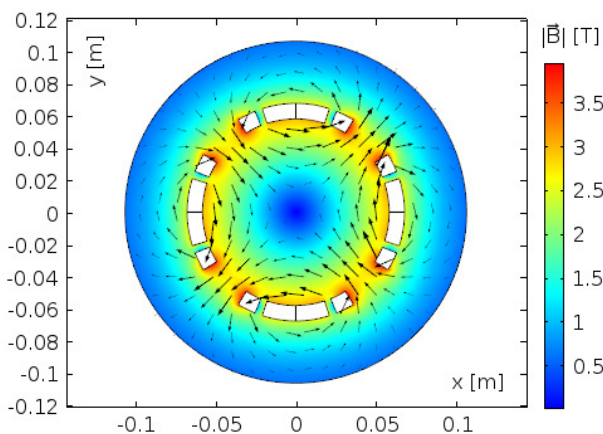


Figure 5: Quadrupole magnetic field distribution within the transverse cross-section plane.

## Combined-Function Magnet

Adding up a dipole field pattern obtained for 1 T peak field with a quadrupole field pattern obtained for a gradient of 25 T/m yields the field distribution shown in Fig. 6. If the dipole coils are tuned for a given beam energy such that the path coincides with the magnet geometrical centre, beams of higher energy will deviate towards the higher dipole field region and be bent along the gantry on an off set wiggling path. Similarly, beams of lower energy will be deviate towards the lower field region and travel along the gantry. An equivalent description is true for the quadrupole field component whose focusing strength shows a gradient transversely. Therefore, unlike individual dipole or quadrupole magnets which either bend or focus for a narrow energy range, the combined-function magnet does both for a much larger energy range.

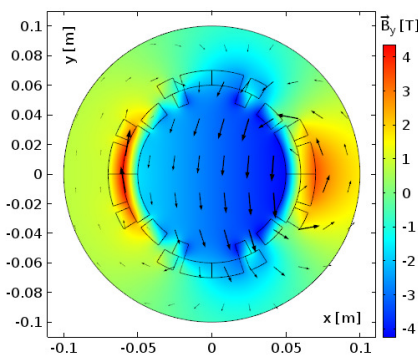


Figure 6: Bending magnetic field generated by the combined-function magnet in the transverse cross-section.

## STEERING SYSTEM

Particles finish their path at a height of 2.50 m above the isocentre and need to be focused and scanned across a 30 cm  $\times$  30 cm target area which is placed 195 cm below. A beam scanning system must be designed to achieve this operation with high precision. This is intended to use normal conducting technology for the magnets and thus forms a distinct mechanical assembly outside the cryostat. In its simplest form it can be designed using two quadrupole and two dipole magnets, as shown in Fig. 7. The quadrupoles are required in order to continue the transverse focusing of the gantry lattice while the beam is carried to the target, but one of the most important aspect is their possibility to tune the size and orientation of the irradiated area, modulating the beam intensity within its transverse cross-section.

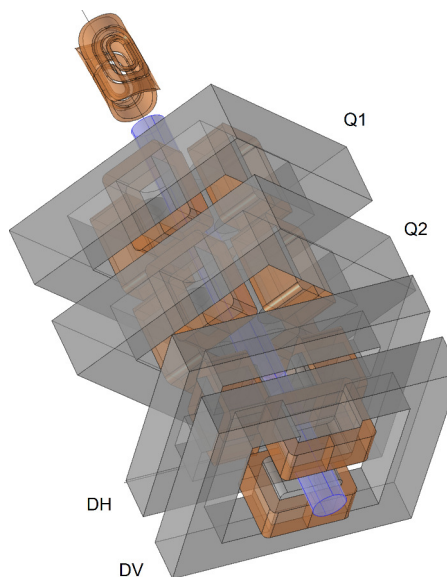


Figure 7: Preliminary assembly of the beam steering system installed on a 1 m long beam pipe.

Target scanning on a grid of 2 mm  $\times$  2 mm can be seen in Fig. 8 for 250 MeV. At this energy, the magnetic field change is 13.2 mT/mm for the horizontal scanning and 11.4 mT/mm for the vertical scanning.

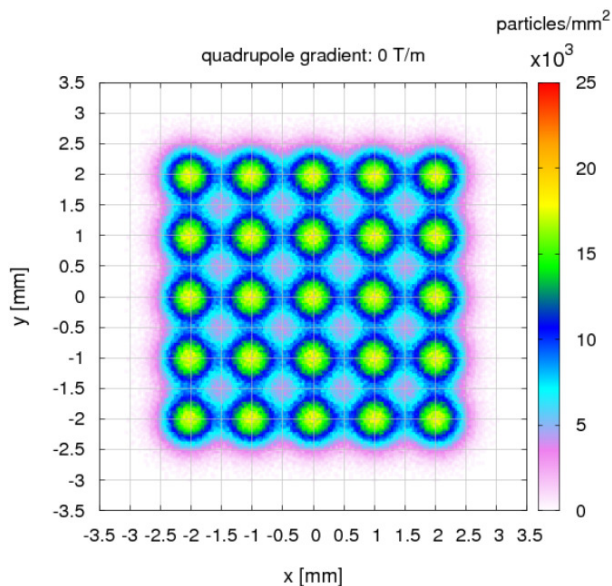


Figure 8: Beam position scanning for  $10^4$  particles at the target for 250 MeV using the two dipole magnets with zero quadrupole gradient.

However, at 100 MeV the magnetic field change is 8.10 mT/mm for the horizontal scanning and 7.4 mT/mm for the vertical scanning; this should be considered as the degree of sensitivity required.

### PARTICLE TRACKING

Particle tracking studies have been carried out using the specialized GPT code [6] with magnetic field maps obtained externally. At the current status of the project only methods to check the transmitted beam energy range have been implemented as one example can be seen in Fig. 9 with field values evaluated for a few energy ranges in Table 1.

Table 1: Energy Range and Corresponding Magnetic Fields

Energy range [MeV]	Dipole Field [T]	Quadrupole Field gradient [T/m]
200 - 250	2.195	90
170 - 220	1.891	85
130 - 165	1.740	40
100 - 150	1.575	60

### CONCLUSIONS

A preliminary lattice made of combined-function magnets has been designed with the purpose to study proton beam dynamics through realistic field maps. Current results show that 250 MeV beams can be handled with dipole fields of about 2.2 T and quadrupole field gradients of about 90 T/m.

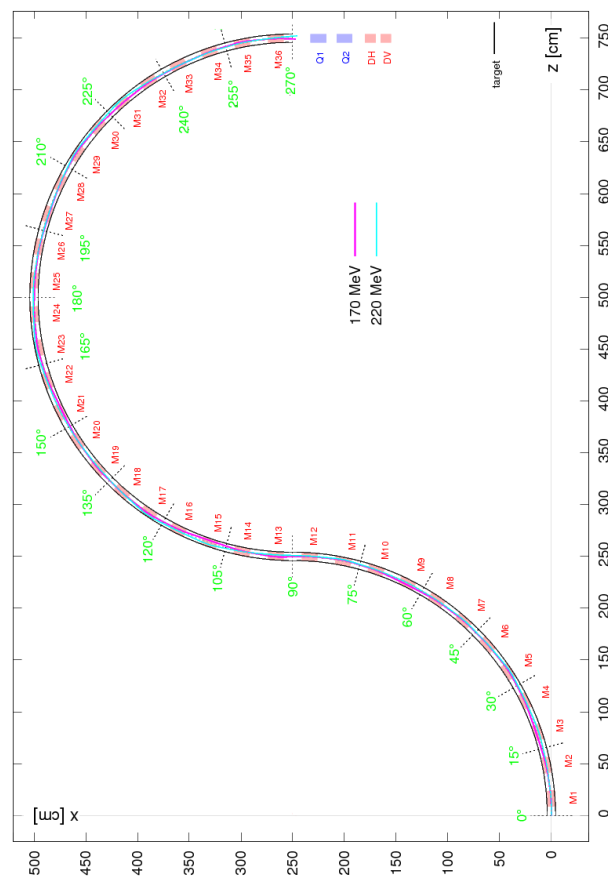


Figure 9: Trajectories of two proton beams of 170 MeV and 220 MeV respectively.

However, the energy range which can be transported at fixed field is no more than 50 MeV. Further modelling work is necessary in order to increase this range and efforts are directed towards coupling magnetic fields with particle tracking directly in Comsol in order to avoid errors which arise when field maps are truncated and processed externally.

### REFERENCES

- [1] D. Trbojevic et al., Phys. Rev. ST Accel. Beams, 10:053503 (2007).
- [2] C. Bontoiu et al., “Design of a Superconducting Gantry Cryostat”, IPAC’15, Richmond, USA, May 2015, WEPMN051, These Proceedings.
- [3] Comsol website: <http://www.comsol.com/products/multiphysics/>
- [4] L. Rossi et al., Phys. Rev. ST Accel. Beams, 10:112401 (2007).
- [5] L. Rossi et al., Phys. Rev. ST Accel. Beams, 9:102401 (2006).
- [6] GPT website: <http://www.pulsar.nl/gpt/>

Content from this work may be used under the terms of the CC BY 3.0 licence (© 2015). Any distribution of this work must maintain attribution to the author(s), title of the work, publisher, and DOI.